Soft Matter

Accepted Manuscript

ROYAL SOCIETY
OF CHEMISTRY

www.rsc.org/softmatter

Received 00th January 20xx,
Accepted 00th January 20xx

DOI: 10.1039/x0xx00000x

www.rsc.org/

Formatting – please delete this box prior to submission

- Graphics, including tables, will be located at the top or bottom of the column following their first citation in the text during production (unless they are equations, which appear in the flow of the text). They can be single column or double column as appropriate and require appropriate captions.
- Text is not wrapped around any of the graphics.
- During production, sufficient space will be inserted around graphics for clarity of reading; a horizontal bar will also be used to separate all inserted graphics, tables and their captions from the text:
- Please consult the Styles menu for recommended formatting for all text, including footnotes, references, tables, images and captions.

---

[a] *Centro de Física de Materiales (CSIC-UPV/EHU), Paseo Manuel Lardizabal 5, 20018 San Sebastián, Spain*
[b] *Departamento de Física de Materiales, Universidad del País Vasco (UPV/EHU) Apartado 1072, 20080 San Sebastián, Spain*
[c] *Donostia International Physics Center, Paseo Manuel Lardizabal 4, 20018 San Sebastián, Spain*

† Footnotes

Dielectric relaxation of polymers: segmental dynamics under structural constrains

Angel Alegria,[a, b] and Juan Colmenero, [a,b,c]

Abstract: In this article we review the recent polymer literature where dielectric spectrosocpy has been used to investigate the segmental dynamics of polymers under the constrains produced by self-structuring. Specifically, we consider three show cases: i) semicrystalline polymers, ii) segregated block-copolymers, and iii) asymmetric miscible polymer blends. In these three situations the characterisitics of the dielectric relaxation associated with the polymer segmental dynamics is markedly affected by the constrains imposed by the corresponding structural features. After reviewing in detail each of the polymer systems, the most common aspects are discussed in the context of the use of dielectric relaxation as a sensitive tool for analyzing structural features in nanostructured polymer systems.

Introduction

Polymers are an important subfamily of the so-called glass-forming materials where crystallization during cooling does not occur or it can be avoided by using a sufficiently high cooling rate. These materials are liquids at high temperature that become solid-like glasses below a certain temperature range, which is known as the glass transition (or more accurately liquid to glass transformation). [1-5] The molecular dynamics responsible for maintaining thermodynamic equilibrium of the system becomes gradually slower during cooling to the glass transition range, so when the time scale of the molecular rearrangements required to maintain the thermodynamic equilibrium is of the order of the reciprocal of the cooling rate the liquid can no longer maintain the thermodynamic equilibrium and the material becomes a glass. Since this increasing of the time for molecular motions occurs very abruptly, a single temperature, T_g, usually characterizes conveniently the glass transition, although the transformation occurs in a temperature range of a few degrees [1-5]. When a glass-forming material is heated above the glass transition crystallization can occur. In polymer materials this crystallization process is known as cold-crystallization since usually it takes place far below the melting temperature. The cold-crystallization process is kinetically controlled by the diffusion of the monomeric segments, thus it is also very much related to the above-mentioned molecular rearrangements [6].

Macromolecules are complex objects, which has a clear impact on the molecular mobility. The motions of segments of the polymeric chain, each typically consisting of a few monomeric units, are responsible of the glass transition of polymers [7]. So the segmental dynamics of a polymer at T_g involves times in the range of a few seconds. However, at this temperature other dynamical processes also exist [8]. Particularly, those faster motions responsible of the local changes in backbone chain conformations and/or side chain groups; and those involving the large scale chain motions. These larger scale motions are much slower than the segmental dynamics, the difference increasing dramatically with increasing molecular weight. They are involved in chain end-to-end distance fluctuations and chain center of mass diffusion as well, both related to the polymer flow behavior [7,8].

The molecular mobility is generally investigated by means of relaxation techniques [9]. Relaxation techniques use the response of the material properties to external fields. When the perturbation is weak, the evolution of the material properties is uniquely controlled by the thermodynamic spontaneous fluctuations in the system, and therefore yields information about the molecular mobility of the material [10]. The most prominent relaxation process in glass-forming materials in general is that related to the molecular dynamics controlling the glass transition, i.e. the segmental dynamics in the polymer case [11]. This main relaxation process is often referred to as α–relaxation, whereas those faster relaxations are named with other Greek letters β, γ, ... , and , as a whole, they are referred to as secondary relaxations [12]. The slower main chain motions are responsible of the mechanical relaxation processes reflecting the viscoelasticity of polymeric materials, which are usually named terminal relaxation [13].

The α–relaxation process shows a series of universal features that are observed in most glass forming liquids, including polymers [14]. The most prominent one is the super-Arrhenius temperature dependence of the relaxation time that tends to diverge at a finite temperature located a few ten degrees below T_g [15]. This implies that one have to explore a huge frequency range to detect the α-relaxation in the relevant temperature range, ca. from T_g to T_g +100 K. Other very important feature of the α–relaxation is that the relaxation function is in general non-exponential (non-Debye character) [16] and not much affected by changes of temperature in this relevant range. As a consequence, the time-temperature superposition principle [17] can be often applied as a reasonable approximation. The shape of the α–relaxation is quite similar in most of the systems with a extended short time tail of the relaxation function that is generally well described by the so-called stretched exponential function [18] with a value of the stretching parameter (β, see Technical information section) in the range 0.4-0.6 (a value 1 of the stretching parameter corresponds to a single exponential decay). This makes the frequency range where the relaxation process is relevant at a given temperature to be extended to about 3-4 decades in frequency/time [19]. All these characteristics of the α-relaxation are quite different from those found for the secondary relaxations. As a general rule, the secondary relaxation times show Arrhenius temperature dependence with relatively low activation energy and a quite symmetric stretching of the relaxation function, which increases rapidly as temperature decreases [20].

Among the different relaxation techniques used for the investigation of the polymer dynamics, those detecting the dielectric relaxation [21] are very suitable since most of the polymers have permanent molecular dipole moments in the monomeric unit. In this case, the segmental dynamics of a polymer is detected through the spontaneous fluctuation of the dipole moments in the monomeric units. In particular using broadband dielectric spectrometer, BDS, a range of 10 decades in frequency can be explored in a single setup and up to 16 decades by combining different equipments [22]. In addition, BDS techniques are extremely sensitive and allow detecting very weak relaxation processes. Thus, it is possible investigating either, materials having very small dipole moments, or a given polar polymer as a minority component in a mixture or composite material. A more detail description of the dielectric relaxation fundamentals and some experimental aspects can be found below in the 'Technical Details' section.

The effect of confinement on the material properties is a field with huge activity nowadays [23,24], which is mainly motivated by both, the increasing technological trend towards miniaturization approaching the nanoscale and the concomitant development of nanostructures [25]. In this context the interest of studying the effects of confinement on the polymer dynamics arise naturally [26]. In addition, fundamental investigations on the finite size effects on the α–relaxation look for addressing the ultimate origin of the peculiar universal characteristics of this main relaxation process aforementioned. However, an utmost important factor affecting the molecular dynamics is the direct effect of interfaces when confining polymers by different means [27].

In this review, we will limit ourselves to the particular cases where the material structures are responsible for imposing constrains in molecular mobility, which, as will be shown, arise from various factors. Therefore the reader should not expect to see much reference to the large activity devoted during the last years on the effect of confinement on polymer subjected to 'external' restrictions, as can be the case of polymer films [28] or polymers incorporated inside the nano-scale spaces of nanostructured materials [29]. Rather, we will review the results obtained in some canonical systems where the intrinsic structures of the polymeric material are responsible for constrains. These three kinds of materials are: i) semicrystalline polymers ii) nanostructured block-copolymers iii) polymer blends with large dynamical asymmetry.

The objective of this review is to provide a general description of the structural constrains in these particular materials highlighting the common features of their dielectric α-relaxation and also its specificities. The review is organized as follows. In the next section the dielectric α-relaxation in semicrystalline polymers is described, and the dramatic increasing of the dynamic heterogeneities is discussed in terms of the so called constrain amorphous phase (where the mean segmental mobility is markedly slowed-down) and the rigid amorphous phase (where it would be eventually suppressed). In the next chapter the case of nanostructured block copolymers is presented, making it evident the effect of the interfaces on the dielectric α-relaxation of the block components. Here clear differences are found when comparing that of the flexible one with that of the rigid one. The case of asymmetric miscible polymer blends is presented in the next chapter where the factor responsible for constrains in these single-phase systems is the large dynamic asymmetric between the components. A conclusion section is included summarizing the presented results and emphasizing the common aspects of the dielectric α-relaxation under structural constrains. Finally, a technical section is added at the end, which is intended for the readers without a sufficient background on dielectric relaxation techniques [22].

Dielectric relaxation of semicrystalline polymers

It is very difficult - if not impossible - to obtain polymers in a fully crystallized state. Thus, when glassy polymers crystallize a rather complex nanostructure is generated. The more generally accepted view of the nanostructure of semicrystalline polymers consists in a periodic stack of crystalline lamellas separated by disordered regions (see scheme in Figure 8 of ref [30]) with a rather well defined periodicity. Furthermore, there is a larger structure where these lamellar entities are organized in fibrils giving rise to even bigger structures as spherulites [31]. Thus, the amorphous phase of semicrystalline polymers is in general composed by chain portions of different length fixed by the two ends to crystalline lamellas. Some of the chain portions remain as part of the lamella staking in-between parallel crystalline layers and the rest fill the space among crystallites. As a consequence, once above the glass transition but below the melting range, very heterogeneous segmental polymer mobility should be expected. In general, the segments close to the anchorage points will move slower and besides they will present a sterically reduced ability for reorientation. The dielectric relaxation results confirm these expectations. As a general rule, the characteristic relaxation time (reciprocal of the angular frequency at the maximum of the dielectric loss peak) of the α–relaxation in semicrystalline polymers is larger by more than one decade than that measured at the same temperature in the fully amorphous material.

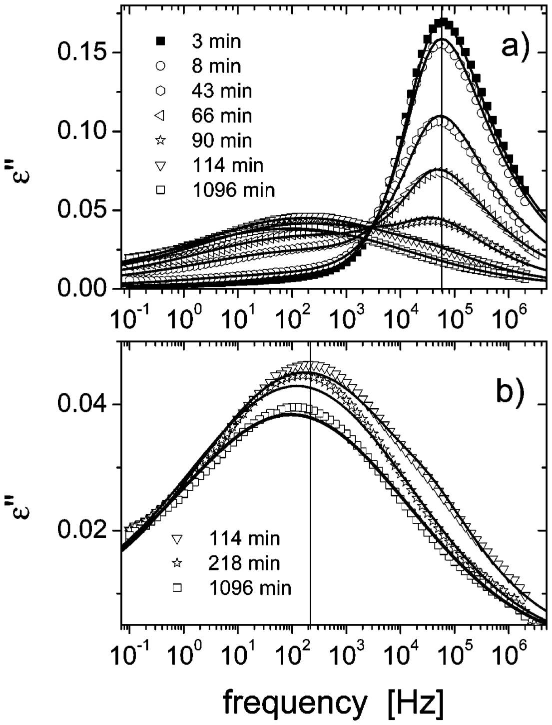

FIGURE 1. Dielectric losses of the α–relaxation of PDMS recorded at 162 K during cold-crystallization of an initially amorphous sample. Frame b) highlights the evolution at long times. Reprinted with permission from ref. [32].

This is nicely illustrated in Figure 1 where the dielectric losses of poly(dimethylsiloxane), PDMS, recorded in the course of crystallization at 162 K are presented [32]. The dielectric relaxation of the fully amorphous polymer presents a loss peak with the typical features of glass forming liquids, that is: i) full-width at half-maximum (FWHM) of about 2 times larger than the 1.14 decades corresponding to a Debye relaxation process (exponential decay in time domain) and ii) a broadening markedly more pronounced in the high frequency side. This 'spectral shape' is characteristic of a stretched exponential decay of the corresponding time domain relaxation. At the first stages of the crystallization process the main dielectric loss peak decreases in intensity maintaining the peak frequency constant and without much change in shape, whereas a new relaxation contribution at markedly lower frequencies becomes apparent. As crystallization develops, this evolution continues in such a way that there is a frequency at which the dielectric losses remains unaltered (the so called isosbestic point) indicating that the measured response can be accounted by the superposition of two distinct components that are interchanged during the time evolution. The chain segments incorporated in the polymer crystalline phase cannot give rise to a measurable dielectric relaxation. Thus, in this regime the conventional amorphous phase that is lost is in part transformed in a new amorphous phase. This distinct phase is usually known as 'constrained amorphous phase' (CAP) [33]. The corresponding dielectric losses are not only showing a peak shifted to lower frequencies but also show up as an extremely broad peak with a FWHM larger than 4 decades. This characteristic can be attributed to the dynamic heterogeneity associated to the different segmental mobility in the new amorphous phase separating the crystalline lamellas in the layered nanostructure and/or that between the lamella stacks forming other superstructures. It is worth mentioning that a similar phenomenology has been reported for side group crystallization in poly(n-octadecyl methacrylate) [34].

An interesting aspect that has not been investigated in detail is the fact that being the overall dielectric relaxation of the amorphous phase much slower than that of the conventional amorphous polymer melt the loss curves of the former still present very significant contributions at the high frequency tail. For example, by comparing the dielectric losses of fully amorphous and cold crystallized PDMS at a temperature where the loss peak occurs at around 30 Hz (152 K and 160 K respectively) what is found is that both data sets merge in the MHz range (see Figure 8 in ref [32]). Due to the fact that the amount of amorphous phase is reduced in partially crystalline polymers, this implies that in the amorphous phase constrained by the neighboring crystalline lamella there is a relatively higher amount of fast moving dipoles. The origin of such situation can be related with the fact that constrains imposed by the crystalline regions, avoid an efficient packing of the surrounding amorphous material. This would generate a significant heterogeneity in local density/packing with relatively high population of badly packed chain segments, which would present a higher mobility. On the contrary, there will be also segments in the very vicinity of the crystalline lamella, that belong to the chain potions where anchorage to the crystals is relevant, which will be forced to closely pack and they will present a slower than average segmental dynamics. This heterogeneity of the segmental mobility in the constrained amorphous phase of semicrystalline polymers would easily explain the extremely broad dielectric α-relaxation loss peak. However, the situation qualitatively changes during the later stages of the crystallization process where no significant contributions of the conventional amorphous phase remain and a reduction of the signal from the constrained amorphous phase is clearly visible, which is accompanied by a noticeable shift of the loss peak maxima to even lower frequencies. This behavior is what could be expected by assuming that once the formation of well developed crystalline lamellas is not longer possible some slower process of (likely imperfect) crystallization occurs in the inter-lamellar spacing, which would be more probable in the less restricted parts of the new amorphous region. Thus, a decreasing of the contributions to the dielectric losses at higher frequency would occur. Consequently, at the final stages of the crystallization process the remaining dielectric relaxation loss peak is broad and with a clear asymmetry extending more towards the low frequency side and the average mobility results reduced. With respect to the above picture on the development of polymer crystallization, it is noteworthy that recent NMR results show evidences of interchange of segments between the crystalline and amorphous regions for polymer crystallized form solution [35]. This exchange could influence the dynamic heterogeneities at the segmental level and thus lead to extra features in the dielectric relaxation behavior. However, the fact that such exchange is not of much relevance in melt-crystallized polymers makes it difficult to address this issue.

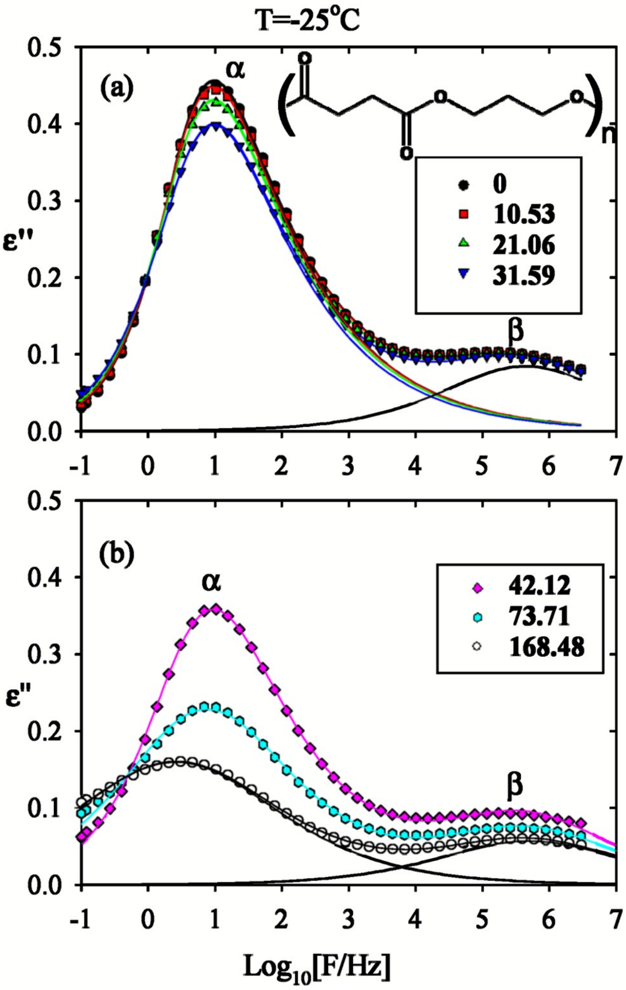

FIGURE 2. Evolution of the dielectric relaxation of poly(propylene succinate) during cold-crystallization. In this polymer the α– and β–relaxations can be both monitored simultaneously on the course of crystallization. Reprinted with permission from ref. [36]

All the previously described phenomenology is in agreement with the commonly accepted picture for the crystallization of relatively simple polymers [36-39]. Figure 2 shows, as an example, the evolution of the dielectric relaxation of poly(propylene succinate) (PPS) during cold-crystallization. In this figure the evolution of both the dielectric α– and β–relaxations is observed. Whereas the changes in the former are similar to those shown above for PDMS, the β–relaxation loss is just reduced in intensity without any discernible change in position or shape. This shows that the very local molecular mobility is not noticeably affected by the structural constrains induce during cold-crystallization, which was already established thirty years ago [39].

However, the behavior of semicrystalline polymers with relatively complex chemistry of the monomeric unit is somehow different. As an example, Figure 3 presents the evolution of the dielectric losses of Polyether ether ketone, PEEK in the course of crystallization [40]. In this polymer a more gradual evolution of the dielectric losses is observed, without a clear isosbestic point. This behavior suggests that in this kind of polymers the spatial separation of crystallizing and non-crystallized parts is not well developed and, consequently, the material can be described by an intermediate single phase rather than as a microscopic composite of crystallites imbibed in a still amorphous matrix. The situation seems to be even more complicated in some polymers as, poly(trimethylene terephthalate), PTT. Very pronounced changes in peak frequency of the dielectric losses have been reported [37] at the earliest stages of crystallization of this polymer (see Figure 4). This result has been considered as indicative of the occurrence in PTT of a mesophase state as precursor of crystallization.

A common aspect of the dielectric α–relaxation of crystallized polymers is related with the relation between the dielectric relaxation strength and the amorphous polymer fraction. In a naïf description one would expect the dielectric relaxation strength to be approximately proportional to the amorphous polymer weight fraction since the dipolar units incorporated in the crystalline phase are not longer able to contribute to the orientational polarization. However, the actual situation is that the dielectric relaxation strength of the α–relaxation decreases with sample crystallinity much faster than expected by assuming this simple view [39], as illustrated in Figure 5. The mere linear extrapolation of the decreasing of the dielectric relaxation strength as crystallinity increases yields to a situation where the dielectric relaxation strength would vanish for a crystallinity degree much lower than one (about 0.5 for PPT). This points to the idea that not all the amorphous phase in the semicrystalline material contributes to the dielectric relaxation, and consequently, that there would exist a 'rigid' amorphous phase (RAP) fraction [41].

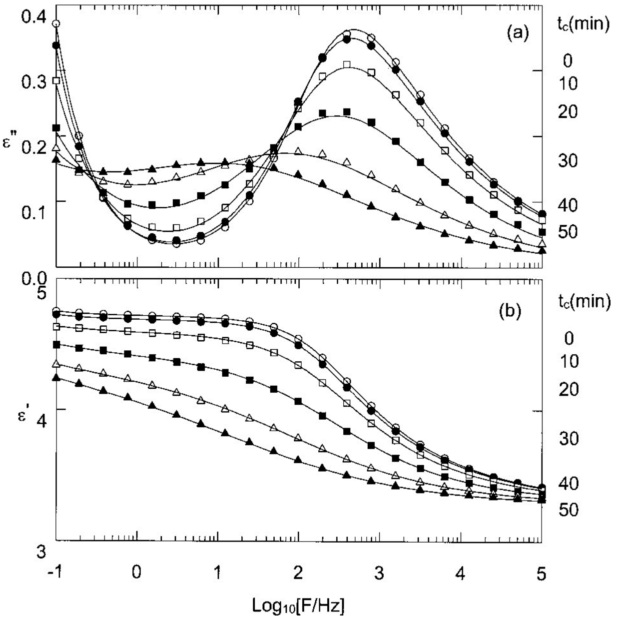

FIGURE 3. Evolution of the dielectric α–relaxation of PEEK during cold-crystallization at 155ºC. Frames (a) and (b) show respectively the imaginary and real parts of the permittivity. Reprinted with permission from ref. [40]

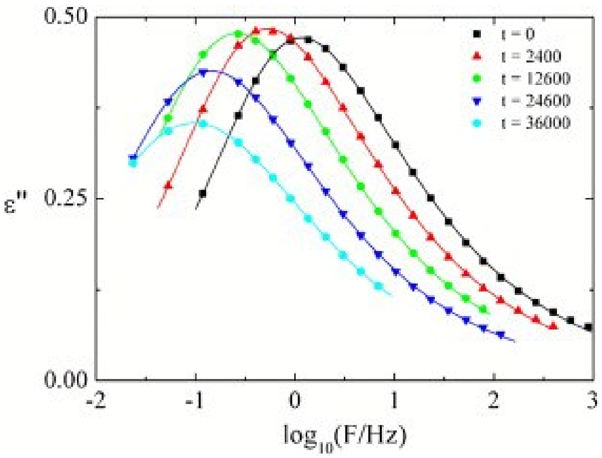

FIGURE 4. Evolution of the dielectric α–relaxation losses during cold-crystallization of PTT at 45ºC. Reprinted with permission from [37]

The RAP existence in semicrystalline polymers was proposed long time ago since a similar situation was found when analyzing the jump of the heat capacity at the glass transition as a function of the crystallinity degree (see ref [43] for a complete description). Although one could easily consider that the mobility of the chain segments of the amorphous phase directly anchored to the crystal surface is very much limited, by dielectric experiments it is very difficult to distinguish between a model of 3-phases (crystalline, RAP and CAP) and a model where CAP and RAP result just from an arbitrary division of the amorphous phase, as recently proposed [42]. In the later case there would be a low frequency long tail of the loss curve that in many cases could be masked by the usual conductivity related contributions in this region. Moreover, the missing dielectric signal could be also interpreted as a restriction in the dipole moment reorientation in the CAP that could be strongly correlated with the relaxation rate, i.e. the more constrain the polymer segment is the slower would it move and more limited its reorientation would be. Furthermore, the dielectric relaxation strength also depends on the extent of the dipole-dipole orientational correlations, which by no means can be assumed to be unaffected by the crystallization process. So, in this picture the RAP would be the limiting CAP case. Literature results on EVA where the crystals are formed by ethylene segments and only vinyl-acetate ones contribute to the dielectric relaxation, point to the fact that the dielectric response of the amorphous phase of semicrystalline polymers present an exceptionally extended tail towards low frequencies, as exemplified in Figure 6. This makes extremely difficult a correct evaluation of the whole dielectric relaxation strength (Δε) of the detected relaxation process, which would be proportional to the area below the loss peak. Consequently, addressing the eventual differences between CAP and RAP is a challenge. In relation with this, it is important to comment that the strength of the dielectric β−relaxation has been found proportional to the amorphous fraction [39] with, as already mentioned, peak frequency and shape not being affected by crystallization (see Figure 2). Therefore, at the local scale RAP and CAP should not be different from that of the conventional fully amorphous polymer.

Summarizing, the dielectric relaxation associated to the segmental dynamics of semicrystalline polymers shows a series of general characteristics that highly the impact of the crystalline phase on the amorphous one. This is particularly enhanced in polymers when compared with low molecular weight glass formers due to the anchorage to the crystallites of the polymer chain fragments forming the amorphous phase,

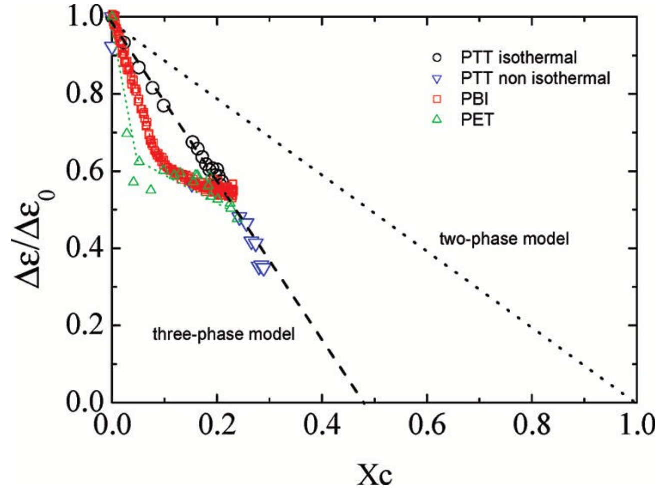

FIGURE 5. Relative change of the dielectric α−relaxation strength as a function of polymer crystallinity for several polymers. Reprinted with permission from [38]

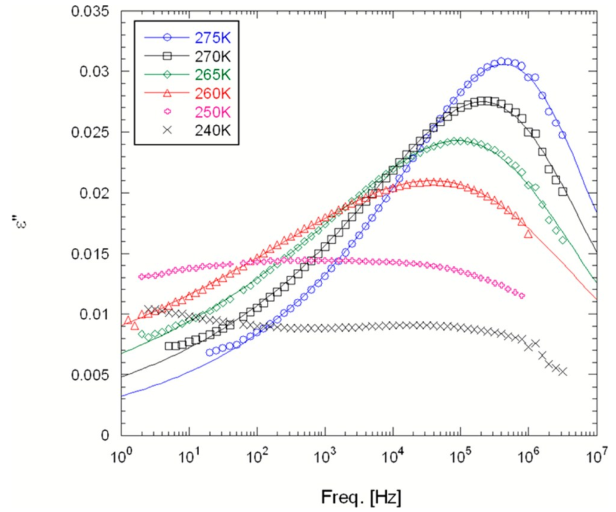

Figure 6. Dielectric relaxation of EVA9 (ethylene-vinylacetate) random copolymer with 9% vinylacetate) as a function of temperatures around the glass transition. Reprinted with permission from [44]

which introduce significant constrains in the mobility of the neighboring chain segments.

Dielectric relaxation of nanostructured block-copolymers

Block copolymers are a class of polymer materials where the individual chains are composed by large portions each formed by a specific monomeric unit [45]. In the simplest case of diblock copolymers, two polymer chains of distinct components are covalently linked by one of the ends resulting in a new linear chain. Depending on the interaction between the chemically distinct monomeric units there would be a tendency for the two components to remain spatially separated giving rise to nanostructures both, in solution and in bulk state. Moreover, in the latter case, the sizes and geometries of these nanostructures can be tuned for a given chemical composition just by selecting the block sizes.

The dielectric relaxation of well-segregated bock-copolymers is in principle originated by the dipole reorientation in the two phases, each of them with characteristics specific of the block components. This is in fact what is found in good approximation when the typical size of the segregated phases is large enough (c.a. lager than some tens nm) [46-51]. A clear example where this view has been found to be valid in a good approximation is shown in Figure 7 where the poly(isoprene), PI, segmental relaxation time determined from the dielectric loss peak frequency in block copolymers of PI and polystyrene, PS, is shown as a function of the PI block molecular mass, and compared with that determined for pure PI.

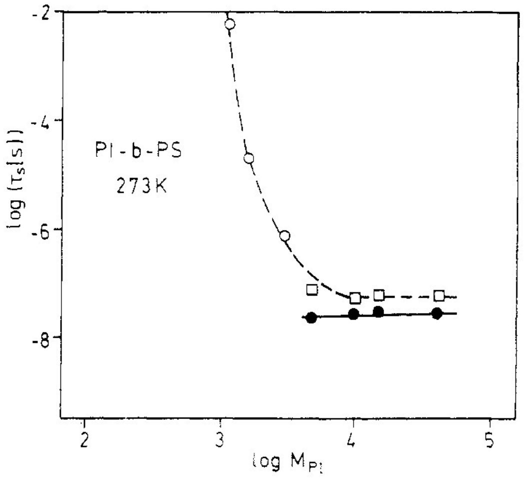

FIGURE 7. Segmental relaxation times of PI in diblock copolymers with polystyrene. The squares represent the results on well-segregated phases and the filled symbols those of PI homopolymers. Reprinted with permission from ref [46]

In Figure 7 it is clearly observed that for high enough molecular mass (i.e. large enough PI segregated phase) the dielectric loss peak frequency detected in the copolymer is nearly the same than that of the pure polymer. However, even in this case, the figure shows that the relaxation times of the fast component in the copolymers is slightly larger than those of the pure polymer suggesting some remaining effect that survive even for the largest sizes. Figure 8 shows that the dielectric relaxation of the more rigid component of block copolymers is also slightly

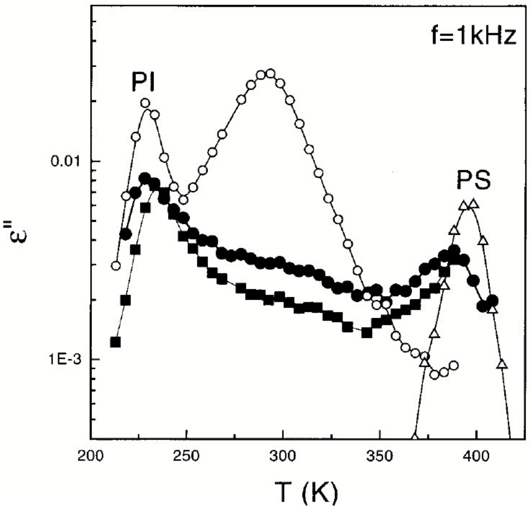

FIGURE 8. Dielectric losses as a function of temperature determined on two phase segregated PS-PI-PS triblock copolymers, in comparison with those corresponding to the homopolymers. Reprinted with permission from ref [48]

shifted, in this case is faster than that of the corresponding homopolymer.

A more recent investigation on the dielectric relaxation in block copolymers of PDMS and PI with varying PDMS block lengths [50] also evidences that for the largest PDMS diblock the dielectric loss peak occurs at similar but slightly lower frequencies than those of pure PDMS having a similar molecular weight (see Figure 9). Similar results have been reported for the faster component in other block copolymers as, PDMS-PI [50], PDMS-PS [51], poly(methyl phenyl siloxane)-PS, PMPS-PS, [53], for instance. In this very early work, [53] it was already clear (see Figure 10) that the loss peak frequency of the resolved contribution from PMPS is substantially reduced respect to that of the homopolymer.

All the discussed results refer to situations in which the temperature range investigated is such that the contribution to the dielectric relaxation of the slower block component is negligible, since the corresponding segregated phase is in a frozen glassy state. There are fewer examples where the dielectric relaxation of the block copolymer is investigated in the temperature range were the slower block component dominates the measured dielectric relaxation. In agreement with what was shown in Figure 8, the results in these cases also evidence a minor shift of the loss peak frequency, now towards higher frequencies, as exemplified in Figure 11 for PDMS-PI block copolymers with different block sizes. In this figure the effect on the loss peak position reflecting the segmental PI dynamics (around 10^5 Hz) is clear and the effect is more pronounced as the size of the blocks decreases (and consequently also the size of the segregated phases). The investigation of the effect at lower temperatures is precluded in these copolymers by the interference of PDMS crystallization. However, PDMS crystallization resulted inhibited in smaller symmetric PDMS-PI diblock copolymers and in these copolymers the dielectric relaxation associated with the segmental PI dynamics can be better investigated over the whole range. As can be seen in Figure 12, the effect on the peak frequency is very clear since in this case the peak frequency is shifted by more than one decade. Here it is also evident that the relaxation peak reflecting the PI segmental dynamics depicted a pronounced high frequency tail, which, however, is at least in part originated by the contributions of PDMS extending towards frequencies much lower than the loss peak maximum of the PDMS component. These relatively slow PDMS contributions are responsible for the increasing losses of the copolymers detected in Figure 12 at high frequencies for the low temperature data from the copolymers.

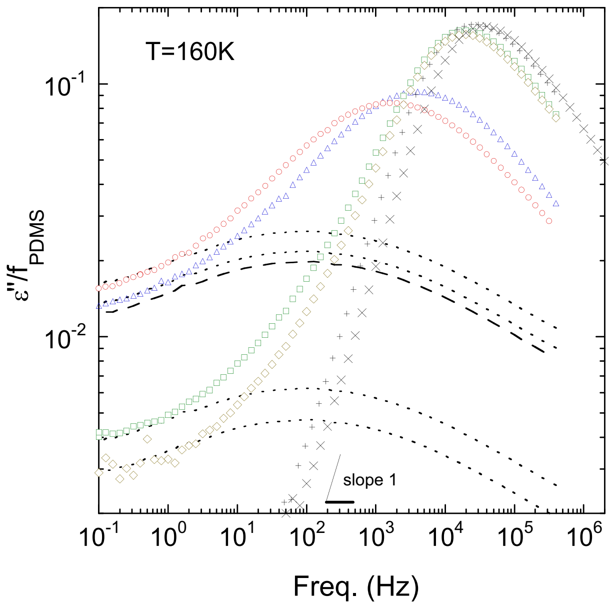

FIGURE 9. PDMS-weighted dielectric losses of various diblock copolymers PDMS-PI with fix size (4 kDa) of the PI block and varying size of the PDMS block 3.5 (circles), 4 (triangles), 23 (squares), and 32 (diamonds) kDa. For comparison de data of a pure PDMS of 3.5 (x) and 21 (+) kDa are included. Lines represent vertically-scaled dielectric relaxation curves of cold-crystallized PDMS at the same temperatures. Reprinted with permission from ref [50]

Despite the relative large number of diblock copolymers investigated so far, analyzing the details of the dielectric relaxation components in these systems is often complicated. Such an analysis requires situations (temperature region, composition, ...) where:
i) the signal coming from the two blocks do not overlap much (dynamic asymmetry and/or much different intensities of the contributions to the measured dielectric relaxation)
ii) negligible conductivity in any of the segregated phases, since the combined effect of ionic conductivity and the presence of interfaces separating the two phases give rise to very prominent interfacial polarization phenomena that hamper resolving the dielectric relaxation related with he segmental polymer dynamics.
iii) structural stability of the segregated phases to allow the comparison of the results obtained at different temperatures/compositions.
These requirements are fulfilled to some extent by PDMS based diblock copolymers. PDMS is a very flexible polymer that as shown above presents a prominent dielectric relaxation associated with the segmental dynamics but nearly undetectable dielectric relaxation below T_g (~150 K) and in most of the cases extremely low conductivity below room temperature.

Although PDMS tends to crystallize below 230 K, crystallization can be easily avoided by fast cooling which allowed investigating the fully amorphous phase of the

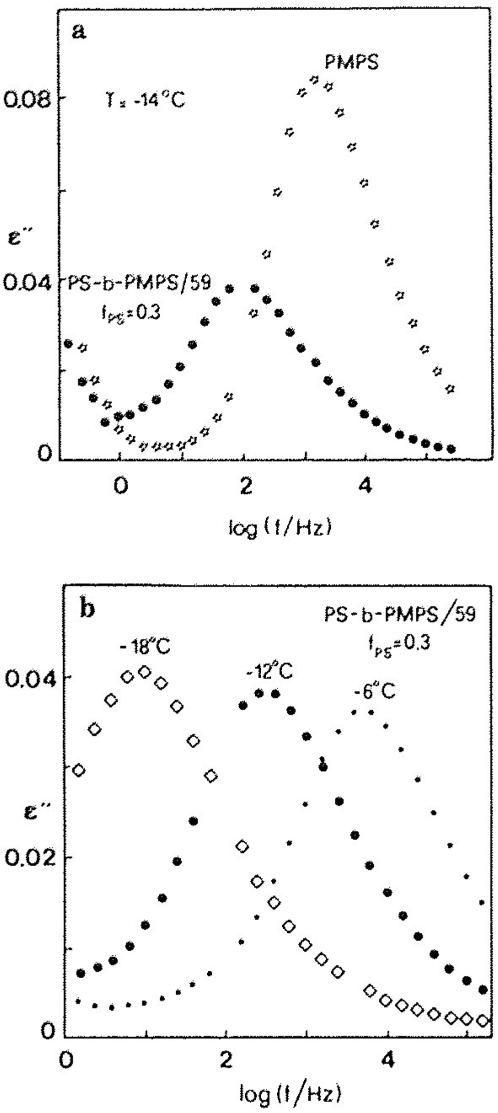

FIGURE 10. Dielectric losses of PS-PMPS block polymer at low temperatures showing the contribution from the PMPS block. (a) Comparison with those of PMPS component. (b) Variation with temperature making evident, at high temperatures, a plateau-like contribution at low frequencies. Reprinted with permission from ref [53]

segregated PDMS at least below 160K, where the dielectric relaxation peak occurs at about 10^5 Hz (see Figure 1 above). Furthermore, for short PDMS blocks, the crystallization of the segregated PDMS phase can be inhibited for symmetric PDMS-PI copolymers, as commented above. The detailed analysis of the dielectric relaxation associated with the segmental dynamics of PDMS in the investigated diblocks [50,51,54] evidence that there are remarkable differences with respect the linear PDMS polymer, in addition of the loss peak shift, mainly in the lower frequency range. Particularly, a plateau-like loss appears, which is more relevant the shorter the PDMS block is, as illustrated in Figure 9. The presence of a plateau-like behavior in the dielectric losses at frequencies much lower than the peak one was not discussed in the early work [53] although data showed clear evidences of it (see frame b in Figure 10).

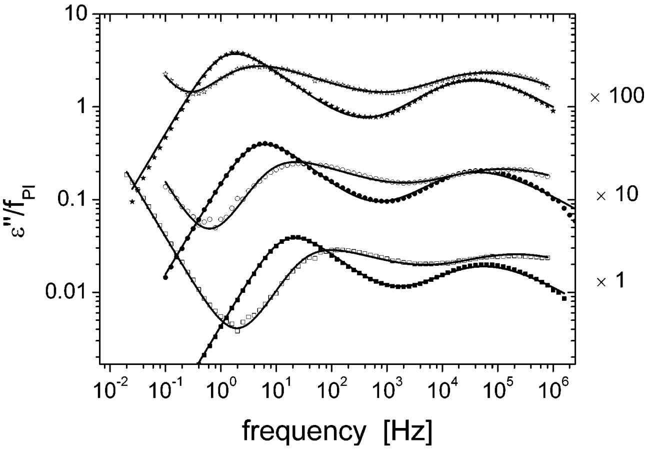

FIGURE 11 PI-weighted dielectric losses of various diblock copolymers PDMS-PI (empty symbols) with approximately fix ratio between PI and PDMS block sizes (PI4-PDMS23, PI6-PDMS31, and PI9-PDMS50) in comparison with the respective PI homopolymers (filled symbols). The faster relaxation component is that related with the α-relaxation whereas de slower one corresponds to the normal mode relaxation, which is not discussed here. Reprinted with permission from ref [49]

Interestingly, the low frequency part of the dielectric losses in the PDMS diblock copolymers can be well compared to that measured in the semicrystalline PDMS at the same temperature. On the basis of these results, it has been proposed [51,54] that such low frequency part of the losses reflects the contributions of the PDMS segments affected by the anchorage of the PDMS blocks to the rigid phase rich in the other component, mimicking in some manner the dynamics of the segments attached to the crystals. This situation would arise because PDMS is one of the polymers with lower T_g and therefore in the range where the dielectric relaxation is accessible the other component is in the glassy state. In Figure 9 it is shown how the measured response on crystallized PDMS matches, after properly scaled in the vertical direction, very well the low frequency part of the measured dielectric losses of PDMS-PI block copolymers (see also figure 6 in ref [51]). Since the segregation geometry of these block copolymers changes (PI is segregated in lamellas, cylinders and spheres when increasing the size of the PDMS blocks) this would be a general behavior reflecting the segmental dynamics of the fully amorphous faster component of diblock copolymers close to its glass transition temperature.

In addition to above discussed effect, the dielectric relaxation of PDMS in block copolymers is also broader at frequencies lower than the peak one. A similar behavior is also evident for the PI-PS copolymers (see Figure 4 in ref [52]), although the contribution to the dielectric loss of the PI normal mode relaxation (related with the fluctuation of the end to end vector of the PI block) precludes an unambiguous assignment of the measured signal in this system. The broadening of the loss peak in the diblock copolymers respect to that of the reference linear polymer has been interpreted as originated by a gradient of segmental mobility, that at least in part would reflect the distinct dynamics close and far from the interfaces. However, molecular dynamic simulations using bead and spring models [50,51] showed that fast and slow moving segments coexist close to the interfaces. This again resembles the situation described above for the dynamics of the amorphous phase in crystallized polymers where a significant high frequency tail contribution is observed. Therefore, the contribution of the fast

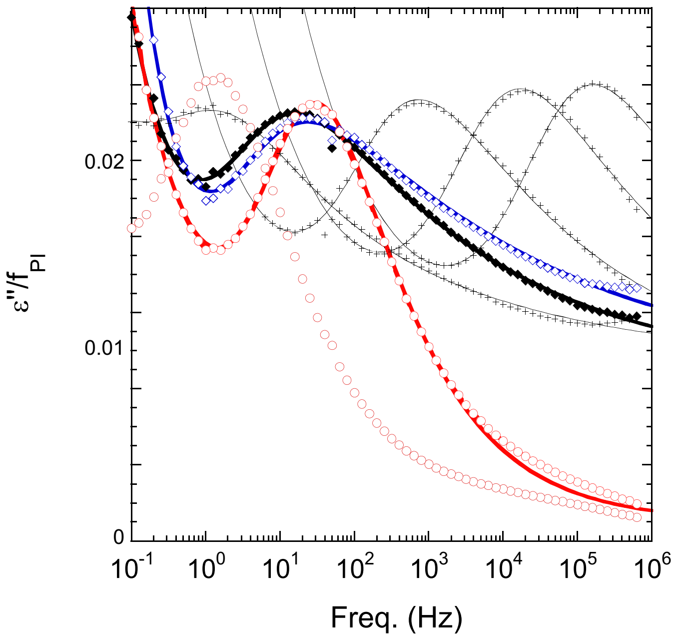

FIGURE 12 PI-weighted dielectric losses at 213 K showing the α-relaxation of the PI component in two nearly symmetric diblock copolymers PDMS-PI: PI4-PDMS4 (filled diamonds) and PI4-PDMS3.5 (empty diamonds). Crosses correspond to PI4-PDMS4 measured a various temperatures (5K steps). Data for PI4 polymer (empty circles) at 213 and 218 K are also shown for comparison. Reprinted with permission from [50]

moving segments close to the interface is likely already captured in the semicrystalline-like component used to account for the low frequency plateau. Thus, the failure of these simulations in detecting a continuous gradient in mobility as we move farer from the interface could be related with the combination of the relatively high temperatures explored and the moderate dynamic asymmetric of the simulated systems. Putting in numbers, on the assumption of a three phase model for the dielectric relaxation of PDMS in PDMS-PS diblock copolymers segregated in lamella phases about 10 nm thick, it was found that about 15% of the segments are strongly affected by the interface, and about 60% would behave as the amorphous linear PDMS (most likely located in the central part of the lamella), the rest (about 25%) likely located in a gradient of mobility region.

The behavior described above is also found in grafted polymers where the anchorage to a solid surface would slow-down, would limit the segmental reorientation and simultaneously would difficult the efficient packing close to the interface. [22,58] These similarities support the high relevance of anchorage in the dielectric relaxation related with the segmental dynamics of the most flexible copolymer block.

Despite that the above description seems to be valid for most of the diblock copolymers there are situations where new phenomena can arise, in particular when a 'closed' segregated phase has a size approaching the nanometer scale. Although such a situation has been scarcely explored, the results obtained on very asymmetric PS-PDMS diblock copolymers with small PDMS blocks evidence these effects [54]. Figure 13 shows the dielectric relaxation of three PDMS-PS diblock copolymers with different segregated geometries and sizes. In the lower panel the previously reported behavior is observed (low frequency plateau and loss peak broadening at frequencies above the maximum which is slightly shifted towards lower frequencies when compared with the reference linear PDMS). However, for the other two diblock-copolymers the situation is different since the loss peak frequency is shifted to higher frequencies and the broadening of the loss curve is also pronounced at higher frequencies.

These results have been interpreted as originated by the defective packing of the PDMS segments in the segregated 'closed' phases. The structural differences were evidenced by complementary experiments by means of Fourier-transform infrared absorption and X-ray diffraction [54]. The ultimate reason for this defective packing would be the miss-match between the thermal expansion of the glassy PS matrix and that

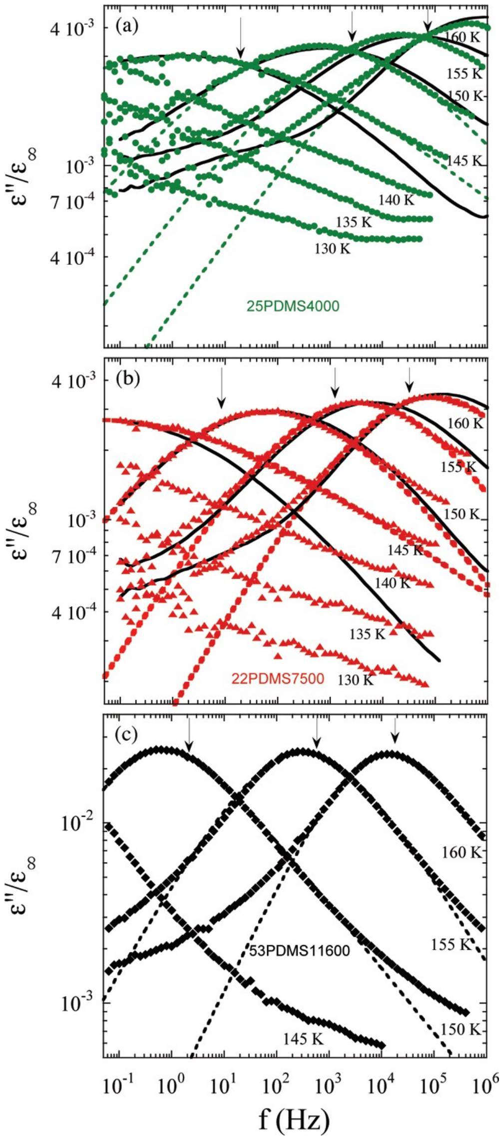

FIGURE 13. Dielectric losses of PDMS α-relaxation in PDMS-PS diblock copolymers with different PDMS segregation geometries. (a) cylindrical, (b) spherical, and (c) lamella. The vertical arrows correspond to the peak position of bulk PDMS with the same molecular weight at 150, 155 and 160 K. Reprinted with permission from [54].

of the segregated PDMS phases. Thus, it seems that the confinement geometry is very relevant for observing these effects since in lamella phases even for small sizes (below 6 nm) the more conventional behavior is observed while for spherical segregation of about 20 nm diameter the effect is very evident (panel b in Figure 13).

Most of the characteristics discussed above are related to the presence of a rigid interface and therefore are relevant for the segmental dynamics of the more flexible block component. The characteristics of the dielectric relaxation associated to the slower component are in fact different. We already showed in Figure 12 that the peak of the loss curve is in this case shifted towards higher frequencies, being the shift smaller as the size of the segregated phase increases. However, it persists for relatively large sizes. In addition the results evidence a significant broadening of the loss curve. When comparing different confining geometries for the segregated phase of PI block of the same molecular weight, the data look quite similar (see Figure 14). Unfortunately the comparison is only possible at a relatively high temperature, where PDMS crystallization did not occurred, and therefore the details of the high frequency side behavior are not visible here. In addition, the normal mode contribution of PI is readily affected by the segregated phase geometry precluding the detailed comparison of the low frequency part of the loss curve associated to the PI segmental dynamics. Overall, the behavior of the different copolymers is similar and the low frequency part of the loss curve is not very different form that measured in the reference linear PI.

For symmetric PI-PDMS diblock copolymers, where the whole relevant temperature range can be explored due to the inhibition of PDMS crystallization, a broadening of the loss curve at frequencies higher than that of the peak is very apparent (see Figure 12). This would manifest the speed up of the segmental mobility of PI (at least close to the interface) induced by the extremely mobile PDMS segments. There would be two major reasons for this, both dictated by thermodynamics. On the one hand, for relatively short blocks there will be a significant number of PI segments in the area of the interface where there exist a composition profile which depends on the Kuhn lengths of the block components and the Flory-Huggins interaction parameter. On the other hand, there would be random stochastic fluctuations producing an additional broadening of the interface. Thus, one would have a region in the interface where there is a partial mixture of segments of the two components explaining the higher frequency contribution to the dielectric relaxation associated with the segmental dynamics of the slower component. Rather simple quantitative approaches based on these ideas have been proposed [48,49] accounting for the experimental results. However, although reasonable values were inferred for the interfacial widths the approach is likely too crude to be used for obtaining quantitative information.

Summarizing, the dielectric relaxation in segregated diblock copolymers show the influence of the interface in the segmental dynamics of each block component with a small effect for large segregated phases. Nevertheless, the dielectric relaxation from the faster component always present a plateau-like losses at frequencies a few decades lower than that of the loss peak maximum, which is originated by the anchorage of the flexible chain blocks to the frozen segregated phases of the other component. Moreover, in addition of a gradient of mobility in the regions close to the interface, the dielectric relaxation also evidences dramatic effects on the segmental dynamics for small closed segregated phases, in particular, for the segregated fast component. This effect is directly related to structural features most likely originated in the packing frustration induced by the miss matching between the thermal expansion coefficients of both phases. As a final remark, it should be taking into account that there are effects other than those here reviewed as for instance those related with the different chain stretching dictated by the degree of segregation [45].

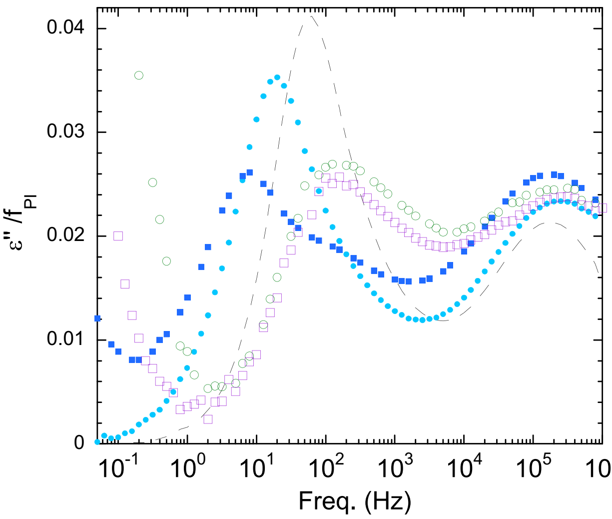

FIGURE 14. Dielectric relaxation at 243 K showing the PI contributions in segregated PI-PDMS diblock copolymers with different segregation geometries, (filled squares and filled circles lamella, empty squares cylinders, and empty circles spheres). The dashed line corresponds to the dielectric relaxation of a PI of the same molecular weight (4 kDa) at 248K. Reprinted with permission from [50]

Dielectric relaxation of asymmetric miscible polymer blends

Polymer blends refer to mixtures of polymer chains of at least two distinct compositions and represent a type of materials which properties can be tailored by selecting the polymer components and concentrations. A subfamily of polymer blends is that of the miscible mixtures. In these mixtures there is an intimate contact between the monomeric units of the two components and the material properties are in general in-between those of the pure components. For example, the glass transition temperature of a miscible blend, as determined by the middle point of the change in heat capacity for instance, is expected to be that calculated with the Flory-Fox equation [59]. However, when considering the segmental dynamics, i.e. that probed by the dielectric α–relaxation, the chain connectivity of polymers is of relevance. The reason is that for the typical length scale involved in the segmental dynamics (a few nanometers) [60] a given component segment of a miscible polymer blend is surrounded in average by more segments of the same type than those deduced from the mean blend composition, i.e. the segments experience an effective concentration different from the macroscopic one [61]. This fact led to the concept of self-concentration [62] that takes into account the volume around a given segment that is occupied by segments of the same chain. This effect is especially important in the case of asymmetric compositions where the polymer of consideration is the minority, since the dynamics of the minority component in the blend is always far different from the dynamics of the majority component in the same blend. When the time scale disparity between the components is huge (large dynamic heterogeneity), for blends with a fast minority component (large compositional asymmetry) the dynamics of the latter can be investigated in a region where the chains of the slow majority component are essentially frozen. Thus, one can view the miscible polymer blend in this range as composed by a vitreous matrix formed by the slow component chains with intricate 'cavities' in which the most mobile component is still moving. Under these circumstances, it would be expected that the segmental dynamics of the fastest component of a dynamically asymmetric miscible polymer blend would be affected by constrains imposed by the majority slower component in a non-trivial way. The most relevant effect observed in the experiments is that the peak of the dielectric loss curve reflecting the dynamics of the lower T_g component in a blend with a high concentration of the slower one can occur at higher frequencies than that of the pure polymer. This result was first detected in blends of poly(vinyl methyl ether), PVME, with PS [65] although previous results on blends of poly(ethylene oxide), PEO, with poly(methyl methacrylate), PMMA, [64] and PVME with poly(2-chlorostyrene) [63] also suggested similar effects.

Figure 15 shows an isochronal representation of the dielectric losses at a low frequency for blends of PVME and PS with varying composition. As concentration of PS increases the loss peak appears at higher temperatures reflecting the expected slowing down of the segmental PVME dynamics due to the presence of less mobile PS chains. However, a low temperature contribution is also developed giving rise to dielectric losses larger (taking into account the PVME concentration) than those of the pure polymer in the same temperature range. Finally at the highest PS content reported (80 wt%) the maximum of the whole loss peak occurs at temperatures below that of the pure PVME.

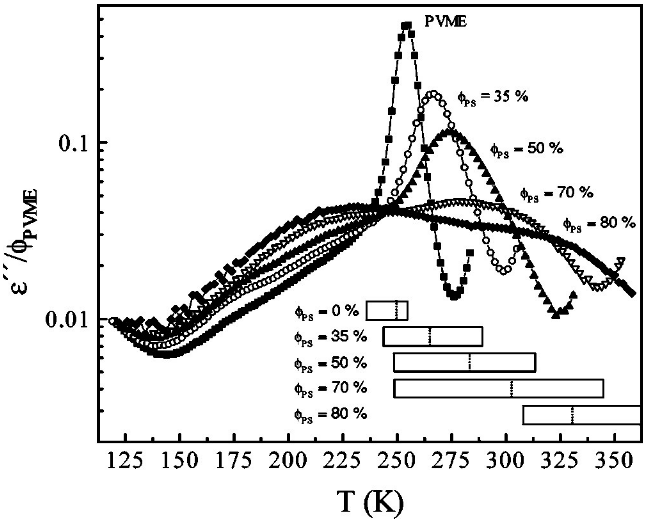

FIGURE 15. Loss dielectric permittivity of PVME at a fixed frequency of 1 Hz as a function of temperature, compared with the dielectric relaxation of blends of PVME/PS. For the comparison the 'dilution effects' on the relaxation intensity are accounted by taking into account the PVME weight fraction in the blends. The bars below indicated the breath of the calorimetric glass transition and the dotted lines the corresponding midpoint T_g. Reprinted with permission from [65]

These results evidence that in PVME/PS miscible polymer blends the dielectric relaxation associated with the segmental dynamics of PVME develops a bimodal character and that when PS is the majority component the relevance of the faster mode in the dielectric relaxation increases markedly and becomes dominant for the highest PS concentration. This phenomenology has been investigated by means of isothermal dielectric relaxation experiments on several compositionally asymmetric blends with large dynamic asymmetry [65-70].

Figure 16 shows the dielectric relaxation associated with the PVME dynamics in the PVME/PS blend with 20 wt% PVME, as a clear example. In these experiments, it was found that the dielectric relaxation of the fast component can be well resolved even below the glass transition temperature range of the blend and that the characteristic relaxation time defined by the peak loss frequency shows Arrhenius temperature dependence below the thermal T_g. However, when the experiments are extended up to temperatures above T_g there is a clear crossover to a more conventional [15] Vogel-Fulcher-Tammann, (VFT) like behavior (see Figure 17). The crossover in the temperature dependence of the relaxation times on heating is also accompanied by a sharp increase of the corresponding dielectric relaxation strength (proportional to the area below the loss curve in Figure 16). This means that at high temperatures approaching the glass transition range, where constrains imposed by the slow blend component would disappear, the dielectric relaxation detected involves the whole PVME dipole reorientation. However, at lower temperatures the full PVME dipole reorientation should occur by some additional slower mode, likely masked in the experiments by the non-negligible contributions of PS.

When interpreting the origin of this phenomenology, it has been proposed that it is related with the emergence of non-equilibrium effects [65], which set-up during cooling as soon as the relaxation time characterizing the segmental dynamics of the slow (high-T_g) component reaches the typical laboratory time, i.e. ~100 s (see Figure 17b). Below this temperature range most of the slow component segments are frozen forming a kind of network, restricting the segmental mobility of the low-T_g component. In this situation, the dipole reorientation is severely limited but also the local environment of the moving segments cannot change much with temperature. The latter implies that the typical segmental dynamics cooperativity that

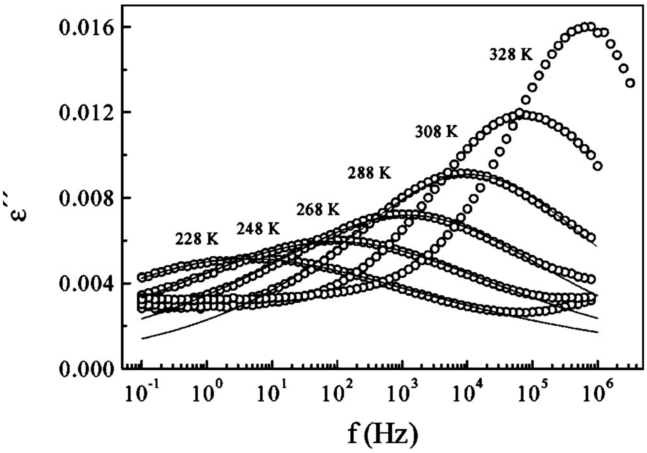

FIGURE 16. Isothermal plots of the frequency dependent dielectric permittivity losses of PVME/PS, with 20 wt% PVME, in the glass transition range. Reprinted with permission from [65]

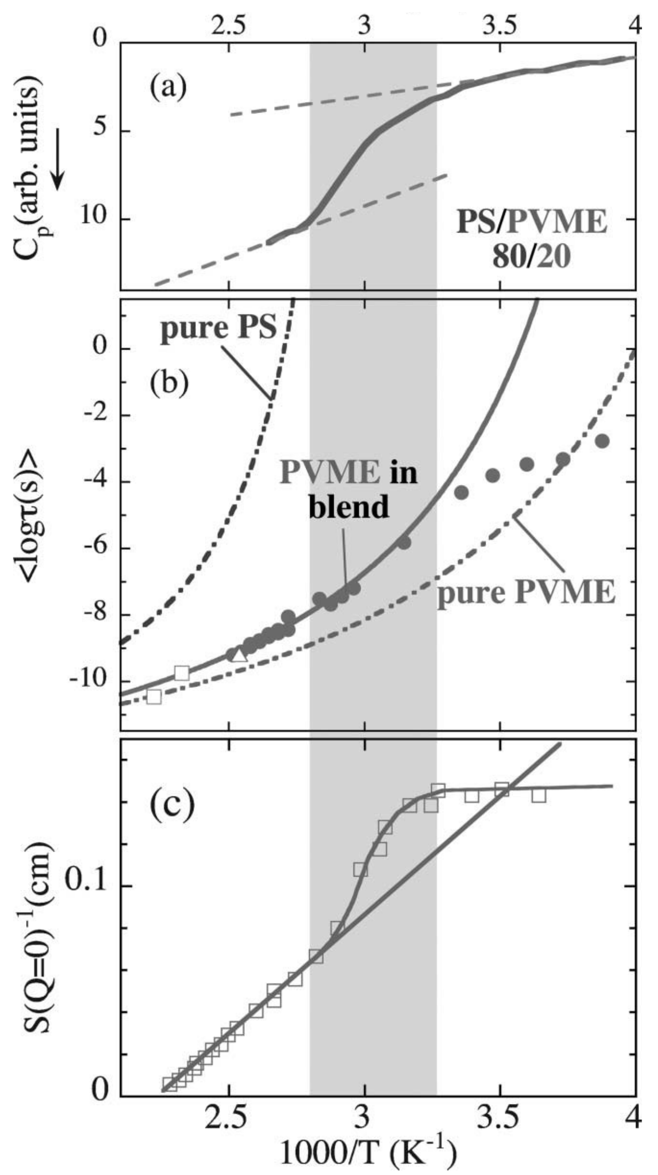

FIGURE 17. Temperature dependence of Cp (a) the main dielectric relaxation time (filled points in b) and the low angle neutron scattering signal measured on PVME/PS blends with 20 wt% PVME when crossing the glass transition range. Reprinted with permission from [66]

normally increases on cooling cannot longer increase, which would explain the crossover towards an Arrhenius temperature dependence below the glass transition of the blend. The large broadening of the relaxation loss curve in this regime would be also a signature of a dramatic dynamic heterogeneity, at least in part generated by the local concentration variations resulting from the freezing of the spontaneous thermal concentration fluctuations (STCF) of the blend. Noteworthy, the STCF are also affected by non-equilibrium effects [66] as soon as temperature decreases below that of the glass transition of the rigid component of the blend (see Figure 17c).

The phenomenology described above is not exclusive of polymers but it has also been found for the dielectric relaxation originated in the reorientation of small molecules [71,72,73]. For example, the characteristic time of dielectric relaxation associated to water in PVME/water mixtures presents a very pronounced crossover in the temperature range where the glass transition of the mixture takes place (see Figure 18). Also results on mixtures of two small molecules (see Figures 19 as a recent result) evidence that the behavior is not specific of polymer based systems and also arises in mixtures of two components with a large dynamical asymmetry. Particularly, by combining dielectric relaxation and Nuclear Magnetic Resonance, NMR, data [73] it has been unambiguously proved that the detected dielectric process reflects the α–relaxation of the faster component under the constrains of the more rigid component and discards the repeatedly proposed scenario that considers that the detected relaxation is just a secondary process reflecting a very local scale molecular mobility [74]. A very elegant demonstration of the non-equilibrium effects on athermal mixtures is the binary blend of PS with oligostyrene, which are perfectly miscible yet dynamically heterogeneous. In figure 3 of ref [75] it can be seen that non-equilibrium effects in the dynamics of oligostyrene in a mixture with 75% PS are quite dramatic.

On the other hand, it has been shown that the constrained dynamics in miscible polymer blends also produces a change in the temperature dependence of the ionic conductivity, which eventually leads to an increase of the conductivity of polymer electrolytes by adding a rigid component. A prove of concept of this phenomenon was reported by investigating the dc conductivity of Li^+ containing PVME/PS miscible blends.

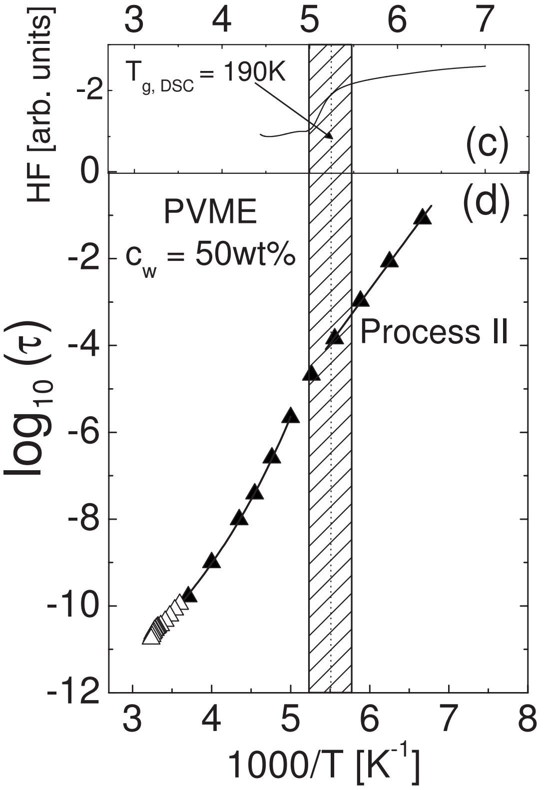

FIGURE 18. Temperature dependence of the DSC trace (upper panel) and the dielectric relaxation times (lower panel) of a 50 wt% mixture of water with PVME. The relaxation times reflect the water specific dynamics in the mixture. Reprinted with permission from [71]

Data in Figure 20 show that the conductivity of Li^+ containing PVME at T_g (250K) is lower than that of blends with 20 and 30 wt% of PS with the same Li^+ concentration at the same temperature, i.e. well below the calorimetric glass transition of the blend.

Although the anomalies in the dynamics of the low-T_g component of miscible polymer blends has been confirmed by means of other techniques [66] as quasielastic neutron scattering (QENS), NMR and also by molecular dynamics simulations, the signature of this behavior on the dielectric relaxation is not always so dramatic. Particularly, the dielectric relaxation of PI in blends rich in poly(terbutyl styrene), PtBS, (with a much higher T_g) is extremely broad but it shows no clear signs of bimodality [77]. Furthermore, any evident crossover in the temperature dependence of the dielectric loss peak relaxation time is directly detectable (see figure 4 in [77]), and in the low frequency range there are significant contributions from both the PtBS segmental dynamics and the PI normal mode relaxation that would mask a low frequency component (if any). However, by analyzing the dielectric relaxation strength of the resolved contribution it is found that it decreases as temperature decreases that would be indicative of constrains, in agreement with the PVME/PS case.
On the other hand, the temperature dependence of the loss peak relaxation time is also weaker than it should be when compared with that of the PI normal mode relaxation (see Figure 21), i.e. it is less sensitive to temperature than that of the normal mode relaxation. This is contrary to that found for pure PI and blends with PI wt% above 50% where both time scales vary similarly at high temperature and approach to each other on cooling close to the glass transition range, which means that the α–relaxation is more sensitive to temperature in this region. Thus, although the crossover in the temperature dependence of the relaxation times is not clear in PI/PtBS blends rich in PtBS, there are experimental evidences of the emergence of several 'anomalies' of the PI segmental dynamics that would be related to the non-equilibrium effects originated on the constrains imposed by the high the component of the blend. Despite of the fact that the above discussed constrain effects on the segmental dynamics of the minority/fast component of athermal polymer blends can be quite dramatic, they already exist in blends containing similar amount of both components [79,80]. In particular, it was found that the high frequency tail of the dielectric relaxation of the fast component presents relaxation contributions faster than those in the pure polymer (see Figure 8 in [79]). The ultimate reason for this would be that the spontaneous concentration fluctuations present in athermal polymer blends induce some regions with local enrichment in the slower component where constrains would exist for the faster component. The amount of such regions increases at higher concentration and consequently their effects are more relevant.

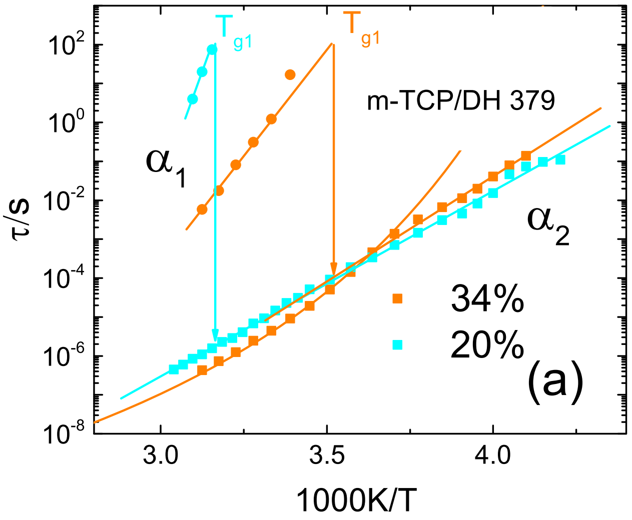

FIGURE 19. Dielectric relaxation times in mixtures of m-tri-cresyl phosphate (m-TCP) and an azobenzene-containing spirobichroman derivative for 20 wt% and 34 wt% m-TCP. Reprinted with permission from [73]

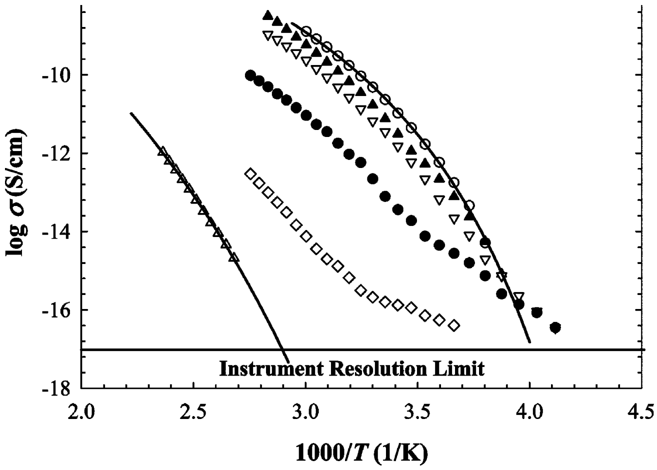

FIGURE 20. Temperature dependence of the dc conductivity of different polymer samples with 1 wt% Li^+. PS (empty up triangles), PVME (empty circles) and blends of PVME/PS with the following PVME content: 10 wt% (empty diamonds), 20 wt% (filled circles), 30 wt% (empty down triangles), and 50 wt% (filled up triangles). Reprinted with permission from [76]

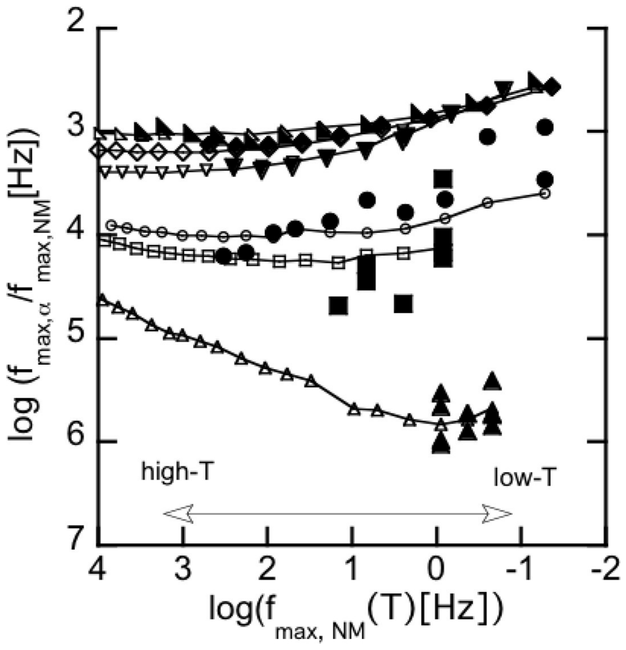

FIGURE 21 Ratio of the peak frequencies of the dielectric alpha relaxation and the PI normal mode relaxation for PI/PtBS blends. Pure PI data appears at the upper part of the plot whereas decreasing PI content in the blend to 80%, 60%, 43%, 35% and 20% results in gradually lower values. The latter behaves very differently. Reprinted with permission from [78]

Summarizing this part, we have shown that the dynamic heterogeneity characteristic of polymer blends where a distinct segmental dynamics of each component exists gives rise to situations where the more mobile component is moving under constrains imposed by an essentially rigid environment. This situation can lead to dramatic changes in the dielectric α–relaxation of the blends, particularly when the low component is the minority but even so it dominates the dielectric relaxation behavior. The main effect is a temperature dependence weaker than expected as temperature is reduced, which in extreme cases would yield to a mobility of the fast component in the blend higher than that of the homopolymer. Interestingly, the large thermal concentration fluctuations characteristic of miscible polymer blends make some similar effects to be relevant also for more symmetric blend compositions.

Concluding remarks

In this review we have presented in some detail how the dielectric relaxation of polymer systems is affected by structural features that introduce some constrains in the segmental motions of polymers. Particularly three different situations have been exemplified. In the case of semicrystalline polymers the constrains arise because the presence of a rigid crystalline phase that, first of all, it reduces the available space, likely giving rise to stresses and density gradients in the remaining amorphous phase. On the other hand the segments of the polymer chains incorporated in the crystals act as anchoring points for the remaining amorphous chain portions. In general this manifests in an overall slower and extremely broad dielectric relaxation that also evidence the presence of highly mobile segments. The second example that we have considered was the situation of segregated diblock copolymers where constrains arise from the dynamic asymmetry of the two phases. The dielectric α–relaxation associated to the segmental dynamics of the more flexible block is mainly affected by anchorage, in a way that resembles what is observed in semicrystalline polymers. When the size of the segregated phase is small, the presence of some mobility gradients is also detectable. However, in some 'closed' segregation geometries, the constrains related with the miss matching between the thermal expansion of the block copolymer components also can give rise to a more dramatic change of the overall dynamics. Finally, we considered the situation of miscible polymer blends where anchorage effects would not to be of relevance but the dynamic asymmetry between the blend-components also imposes constrains on the segmental mobility of the faster component. The major consequence on the dielectric α–relaxation of these systems is the emergence of a component that can become faster than the relaxation in the pure homopolymer, which is a consequence of the constrains arising once the temperature is decreased below the glass transition of the blend. At these temperatures a kind of frozen matrix is developed inside of which there is a significant fraction of mobile segments belonging to the faster component.

Obviously, there are many other situations where structural constrains play a role on the dielectric relaxation of polymer materials. In fact the relaxation behavior can be used to infer the presence of such structural constrains, as it is the case of polymer nanocomposites [81] as a very current example. In fact this approach is being used in many recent publications in different fields. A major difficulty in this method is that the presence of conductive phenomena in structured materials immediately results in dielectric relaxation contributions that can obscure that originated by the segmental polymer dynamics. The microscopic origin of these new relaxation components is not the molecular dipole fluctuations but the diffusion of the electrical charges that eventually become trapped at interfaces [22]. Despite these limitations, investigating dielectric relaxation in polymer materials is a powerful tool to gain insight in the rather complex structural features often present in this important family of materials.

Technical information

A Dielectric spectroscopy

Dielectric relaxation refers to the delay in reaching the equilibrium polarization in a medium after a sudden modification of the electric field. This delay is generated by the 'friction' that opposes to charge displacements and permanent dipole moment reorientations. When in a given material the free charge concentration is extremely low (good insulators) the dielectric relaxation is mainly controlled by the molecular dynamics. Moreover, the linear response theory applies when using low external electric fields and, consequently, the dielectric relaxation reflects the spontaneous dipole moment fluctuations. [21,22]

The simplest model for the dielectric relaxation is the Debye model [22] that considers the reorientation in an uniform electric field of a dipolar sphere imbibed in a viscous medium. In this model the time decay of the polarization, P, after removing the external electric field is given by:

$$P(t) = P(t=0)\ \exp\left(-\frac{t}{\tau}\right)$$

where τ is the so called dielectric relaxation time.

A convenient way to investigate the dielectric relaxation is by measuring the frequency dependent dielectric permittivity. For the Debye model it is given as:

$$\varepsilon^*(\omega) = \varepsilon'(\omega) - i\ \varepsilon''(\omega) = \frac{\Delta\varepsilon}{1+i\,\omega\tau} + \varepsilon_\infty = \frac{\Delta\varepsilon}{1+\omega^2\tau^2} + \varepsilon_\infty - i\frac{\Delta\varepsilon\ \omega^2\tau^2}{1+\omega^2\tau^2}$$

where ε_∞ is the high frequency limit (f≈100 GHz) of the permittivity and accounts for the induce electronic and ionic polarization phenomena responsible for the electromagnetic wave absorptions occurring above the microwave range. $\Delta\varepsilon$ is called the dielectric relaxation strength and accounts for the orientational polarizability of the material. In this equation, the imaginary part of the permittivity reflects the energy losses associated to the dielectric relaxation process, and has a peak shape showing a maximum at the frequency $\omega_m=1/\tau$.

In general, the Debye equation does not describe accurately the experiments that generally show relaxation processes extended over a broader frequency range. A general description of the observed relaxation can be obtained by introducing the idea of a distribution of relaxation times, which yields:

$$P(t) = P(t=0)\ \int_0^\infty g(\tau)\ \exp\left(-\frac{t}{\tau}\right) d\tau$$

$$\varepsilon^*(\omega) = \varepsilon'(\omega) - i\ \varepsilon''(\omega) = \int_0^\infty g(\tau)\ \frac{\Delta\varepsilon}{1+i\,\omega\tau}\ d\tau + \varepsilon_\infty$$

However, the interpretation of the relaxation time distribution function $g(\tau)$ is not unique. On the one hand, different molecular environments would be responsible of the presence in the material of different permanent dipole reorientation rates (dynamically heterogeneous scenario). On the other hand, the reorientation of a given dipole moment could be couple to the environment in a way such that the instantaneous relaxation time is time dependent, being the average behavior of all dipoles equivalent (dynamically homogeneous scenario). In a general case a mixture of both situations could exist.

A different, although mathematically equivalent, approach for accounting of the non-Debye relaxation is by modifying the Debye equation with some empirical parameters. The most generally used of these equations are: the Havriliak-Negami (HN) one, in the frequency domain, and the Kohlrausch-Williams-Watts (KWW), in the time domain. The HN equation reads as:

$$\varepsilon^*(\omega) = \varepsilon'(\omega) - i\ \varepsilon''(\omega) = \frac{\Delta\varepsilon}{\left[1+\left(i\,\omega\tau_{HN}\right)^{\alpha}\right]^{\gamma}} + \varepsilon_\infty$$

where α and γ ($\alpha,\gamma<1$) are parameters determining the peak shape. For $\gamma=1$ the loss peak is symmetric, whereas for decreasing values of α and γ the relaxation becomes broad and asymmetric. The full width at half-maximum (*FWHM*) can be calculated from the shape fitting parameters (α and γ) using the approximate equation [82]:

$$FWHM(\alpha,\gamma) \cong -0.516 + \frac{1.058}{\alpha} + \frac{0.039}{\gamma} + \frac{0.563}{\alpha\ \gamma}$$

The HN relaxation time, τ_{HN}, is related to the loss peak relaxation time $\tau_m = 1/\omega_m$ as [22]:

$$\tau_m = \tau_{HN}\left[\sin\frac{\alpha\,\pi}{2+2\gamma}\right]^{-1/\alpha}\left[\sin\frac{\alpha\,\gamma\,\pi}{2+2\gamma}\right]^{1/\alpha}$$

The KWW equation for the polarization decay is:

$$P(t) = P(t=0)\ \exp\left[-\left(\frac{t}{\tau_{KWW}}\right)^{\beta}\right]$$

where β is called the stretched exponent and the KWW relaxation time is related with the average relaxation time of the corresponding distribution function as:

$$\langle\tau\rangle = \frac{\tau_{KWW}}{\beta}\Gamma\left(\frac{1}{\beta}\right)$$

Some relations have been numerically established for these relaxation functions [83]. The HN equation that represents better the frequency domain counterpart of the KWW one verifies the following relationship between the shape parameters:

$$\gamma \cong 1 - 0.8121\left(1-\alpha\right)^{0.387}$$

In this case HN and KWW parameters are connected as:

$$\alpha\cdot\gamma \cong \beta^{1.23}$$

and

$$\log\tau_{KWW} \cong \log\tau_{HN} - 2.6\cdot\left(1-\beta\right)^{0.5}\cdot\exp\left(-3\beta\right)$$

B. Experimental details

For most of the accessible frequency range (f< 1GHz) the very common sample preparation consists in forming a parallel plate capacitor using two gold-coated metallic discs (with diameter ranging between 10 and 40 mm) as electrodes with a thin (about 50-500 μm) layer of material in between. The frequency dependence of the complex capacitance C^* is determined by means of impedance analyzers or impedance bridges, both using amplitude and phase analysis of the signals. In this way, the complex relative permittivity is straightforwardly determined as:

$$\varepsilon^*(\omega) = \frac{C^*(\omega)d}{\varepsilon_0 S}$$

where ε_0 is the vacuum permittivity, S is de surface of the (smaller) capacitor electrode and d the sample thickness.

Since the dielectric relaxation can be very sensitive to small changes in temperature and moisture in the atmosphere, the sample capacitor is mounted in a cell that is inserted in a cryostat where either a dry high purity gas (Nitrogen or Helium) is used as atmosphere or vacuum is made.

Acknowledgements

The Financial support from Projects MAT2015-63704-P (MINECO/FEDER, UE) and IT-654-13 (Basque Government) is acknowledged.

References

1 C. A. Angell, *J. Non-Crystal. Solids*, 1991, **131**, 13.
2 P. G. Debenedetti, *Metastable Liquids: Concepts and Principles*. Princeton University, 1996.
3 K. Binder (ed.), *Monte Carlo and Molecular Dynamics Simulations in Polymer Science*. Oxford University Press, 1995.
4 R. Zallen, *The Physics of Amorphous Solids.* Wiley-Interscience 1983.
5 W. Kob, *Ann. Rev. Comp. Phys*. 1995, **3**, 1.
6 C. Bhugra, M. J. Pikal, *Journal of Pharmaceutical Sciences*, 2008, **97**, 1329.
7 M. Rubinstein and R. H. Colby, *Polymer Physics,* Oxford University Press. 2009.
8 R.H. Boyd and G.D. Smith, *Polymer Dynamics and Relaxations*, Cambridge University Press. 2007.
9 N. G. McCrum, B. E. Read, and G. Williams, *Anelastic and dielectric effects in polymeric solids*, Wiley, New York, 1991.
10 E.J. Donth *Relaxation and Thermodynamics in Polymers. Glass Transition*. Akademie-Verlag Berlin 1992.
11 I. Gutzow and J. Schmelzer, *The Vitreous State. Thermodynamics, Structure, Rheology, and Crystallization*. Springer-Verlag. 2013.
12 C. Michael Roland, *Viscoelastic Behavior of Rubbery Materials*, Oxford University Press. 2011; Montgomery T. Shaw, William J. MacKnight, *Introduction to Polymer Viscoelasticity*, John Wiley & Sons. 2005.
13 John D. *Ferry Viscoelastic* Properties of *Polymers*, 3rd Edition. 1980.
14 C M Roland, S Hensel-Bielowka, M Paluch and R Casalini, *Rep. Prog. Phys.* 2005, **68**,1405 .
15 H. Vogel, *Phys. Zeit.* 1921, **22**, 645– 646; G. S. Fulcher, *J. Am. Ceram. Soc.* 1925, **8**, 339; G. Tammann, W. Hesse, *Allg. Chem.* 1926, **165**, 254.
16 A. Alegria, J. Colmenero, P.O. Mari, I.A. Campbell, *Phys Rev E,* 1999, **59** 6888.
17 R. M. Christensen, *Theory of viscoelasticity: An introduction*, New York: Academic Press. 1971.
18 R. Kohlrausch, *Annalen der Physik und Chemie* 1854, **91**, 179; G. Williams, G. and D.C. Watts, *Transactions of the Faraday Society,* 1970, **66**, 80.
19 I-S Park, S. Kojima, *Thermochimica Acta*, 2000, **352–353**, 147.
20 J. D. Stevenson and P. G. Wolynes, *Nature Physics* 2010, **6**, 62.
21 CJF Böttcher and P. Bordewijk: *Theory of Electric Polarization*, Verlag Elsevier, Amsterdam, Oxford, New York, 1978.
22 F.Kremer, A. Schönhals (eds.) *Broadband dielectric spectroscopy,* Springer-Verlag, Berlin, 2003.
23 M. Alcoutlabi and G. B. McKenna *J. Phys.: Condens. Matter* , 2005, **17**, R461 .
24 Alejandro J. Müller and Wenbing Hu (eds.) *The Effects of Confinement on Polymeric Thermal Transitions and Nanostructuring*, Progress in Polymer Science, 2016, **54–55**.

25 G.L. Hornyak, H.F. Tibbals, J.Dutta, J.J. Moore, *Introduction to Nanoscience and Nanotechnology*. CRC Press, 2008.

26 Napolitano, Simone (Ed.) *Soft and Biological Matter*, Springer, 2015.

27 A. Budkowski, U. Steiner, and J. Klein, *J. Chem. Phys.*, 1992, **97**, 5229.

28 K. Fukao and Y. Miyamoto Phys. Rev. E 2000, **61**, 1743; V. M. Boucher, D. Cangialosi, H. Yin, A. Schönhals, A. Alegria and J. Colmenero, *Soft Matter*, 2012, **8**, 5119.

29 L. Li, J. Chen, W. Deng, C. Zhang, Y. Sha, Z. Cheng, G. Xue, and D. Zhou, *J. Phys. Chem. B,* 2015, **119**, 5047.

30 A. Pandey, A. Toda, and S. Rastogi, *Macromolecules*, 2011, **44**, 8042.

31 T. A. Ezquerra, A. Nogales, *Polymer Crystallization Obervations, Concepts and Interpretations*, Chap 15 Editors: Reiter, Günter, Sommer, Jens-Uwe (Eds.) Springer, 2003.

32 R. Lund, A. Alegria, L. Goitandia, J. Colmenero, M. A. Gonzalez, and P. Lindner, *Macromolecules*, 2008, **41**, 1364.

33 Sharon Xin Lu, Peggy Cebe, *Polymer*, 1996, **37**, 4857.

34 M. Mierzwa and G. Floudas, *IEEE Transactions on Dielectrics and Electrical Insulation* 2001, **8**, 361.

35 Y.-F. Yao, R. Graf, H. W. Spiess, and S. Rastogi, *Macromolecules,* 2008, **41**, 2514.

36 M. Soccio, A. Nogales, N. Lotti, A. Munari, and T. A. Ezquerra, *Phys. Rev. Lett.* 2007, **98**, 037801.

37 I. Martín-Fabiani, A. Linares, A. Nogales, T. A. Ezquerra, *Polymer*, 2013, **54**, 5892 .

38 A. Sanz, A. Nogales, and T. A. Ezquerra, M. Soccio, A. Munari, and N. Lotti, *Macromolecules* 2010, **43**, 671 .

39 J. C. Coburn and R. H. Boyd, *Macromolecules*, 1986, **19**, 2238.

40 A. Nogales, T. A. Ezquerra, Z. Denchev, I. Šics, F. J. Baltá Calleja and B. S. Hsiao, *J. Chem. Phys.* 2001, **115**, 3804.

41 B. Wünderlich, *Progress in Polymer Science*, 2003, **28**, 383.

42 A. Esposito, N. Delpouve, V. Causin, A. Dhotel, L. Delbreilh, and E. Dargent, *Macromolecules*, 2016, **49**, 4850.

43 C. Schick, A. Wurm and A. Mohammed. *in Polymer Crystallization Observations, Concepts and Interpretations*, Chap 14. Reiter, Günter, Sommer, Jens-Uwe (Eds.), Springer, 2003.

44 M. M. Kummali, A. Alegria, L. A. Miccio, J. Colmenero, *Macromolecules*, 2013, **46**, 7502.

45 Nikos Hadjichristidis, Stergios Pispas, George Floudas, *Block Copolymers: Synthetic Strategies, Physical Properties, and Applications*, John Wiley & Sons, Inc. 2003.

46 I. Alig, F. Kremer, G. Fytas, J. Roovers, *Macromolecules*, 1992, **25** , 5277.

47 A. Kyritsis, P. Pissis, S-M. Mai, and C. Booth, *Macromolecules*, 2000, **33** , 4581; M.L. Yao, H. Watanabe, K. Adachi, T. Kotaka, *Macromolecules*, 1991, **24** , 2955.

48 I. Alig and G. Floudas, A. Avgeropoulos and N. Hadjichristidis, *Macromolecules* 1997, **30**, 5004. G. Floudas, I. Alig, A. Avgeropoulos, N. Hadjichristidis, *Journal of Non-Crystalline Solids,* 1998, **235-237**, 485

49 R. Lund, L. Willner, A. Alegria, J. Colmenero, and D. Richter, *Macromolecules*, 2008, **41** , 511.

50 A. Alegria, R. Lund, F. Barroso-Bujans, A. Arbe, and . J. Colmenero, *Colloid and Polymer Science*, 2014, **292** ,1863.

51 C. Lorthioir, A. Alegria, J. Colmenero, and B. Deloche, *Macromolecules*, 2004, **37** , 7808.

52 G. Floudas, S. Paraskeva, N. Hadjichristidis, G. Fytas, B. Chu and A. N. Semenov, *J. Chem. Phys.*, 1997, **107**, 5502.

53 S. Vogt, B. Gerharz, E. Fischer, *Macromolecules*. 1992. **25** , 5986.

54 L. del Valle-Carrandi, A. Alegria, A. Arbe, and J. Colmenero, *Macromolecules* 2012, **45**, 491.

55 M.Z. Slimani, A.J. Moreno, J. Colmenero, *Macromolecules* 2012, **45**, 8841.

56 M.Z. Slimani, A.J. Moreno, J. Colmenero, *Macromolecules*, 2011, **44** , 6952.

57 S. A. Kim, R. Mangal, and L. A. Archer, *Macromolecules*, 2015, **48** , 6280.

58 N. Neubauer, R. Winkler, M. Tress, P. Uhlmann, M. Reiche, W.K. Kipnusu and F. Kremer, *Soft Matter*, 2015, **11**, 3062.

59 L.A., Utracki, C. A. Wilkie (Eds*.) Polymer Blends Handbook*, Springer 2014.

60 D. Cangialosi, A. Alegria, and J. Colmenero, *Physical Review E*, 2007, **75** , 011514.

61 G.-C. Chung, J. A. Kornfield and S. D. Smith, *Macromolecules*, 1994, **27**, 964; G.-C. Chung, J. A. Kornfield and S. D. Smith, *Macromolecules*, 1994, **27**, 5729.

62 T. P. Lodge and T. C. B. McLeish, *Macromolecules*, 2000, **33**, 5278.

63 O. Urakawa, Y. Fuse, H. Hori, Q. Tran-Cong, O. Yano, *Polymer*, 2001, **42**, 765.

64 M. Dionísio , A. C. Fernandes , J. F. Mano, N. T. Correia, and R. C. Sousa, *Macromolecules*, 2000, **33** , 1002.

65 C. Lorthioir, A. Alegria, and J. Colmenero, *Phys. Rev. E*, 2003, **68**, 031805.

66 J. Colmenero and A. Arbe, *Soft Matter*, 2007, **3**, 1474.

67 A.-C. Genix, A. Arbe, F. Alvarez, J. Colmenero, L. Willner and D. Richter, *Phys. Rev. E*, 2005, **72**, 031808.

68 M. Tyagi, A. Arbe, A. Alegria, J. Colmenero and B. Frick, *Macromolecules*, 2007, **40**, 4568.

69 A.-C. Genix, A. Arbe, S. Arrese-Igor, J. Colmenero, D. Richter, B. Frick, and P. P. Deen, *J. Chem. Phys.* 2008, **128**, 184901.

70 D. Herrera, J.C. Zamora , A. Bello M. Grimau , E. Laredo , A.J. Müller, and T. P. Lodge, *Macromolecules*, 2005, **38**, 5109.

71 S. Cerveny, A. Alegria, and J. Colmenero, *Physical Review E* , 2008, **77**, 031803.

72 S. Cerveny and G. A. Schwartz, A. Alegria, R. Bergman and J. Swenson, *J. Chem. Phys.* 2006, **124**, 194501.

73 B. Pötzschner , F. Mohamed , A. Lichtinger , D. Bock , and E. A. Rössler*, J. Chem. Phys.*, 2015, **143**, 154506.

74 K.L. Ngai, Relaxation and Diffusion in Complex Systems, Springer 2011.

75 V.A. Harmandaris, K. Kremer and G. Floudas, *Phys. Rev. Lett.* 2013, **110**, 165701.

76 D. Cangialosi, A. Alegria, and J. Colmenero, *Macromolecules*, 2008, **41**, 1565.

77 S. Arrese-Igor, A. Alegria and J. Colmenero, *Macromolecules* 2010, **43**, 6406.

78 S. Arrese-Igor, A. Alegria and J. Colmenero, *Macromolecules* , 2011, **44**, 3611.

79 I. Cendoya, A. Alegria, J.M. Alberdi, J. Colmenero, H. Grimm, D. Richter, B. Frick, *Macromolecules* , 1999, **32** , 4065.

80 H. Yang and P. F. Green *Macromolecules*, 2013, **46**, 9390.

81 G. Baeza, C. Dessi, S. Costanzo, D. Zhao, S. Gong, A. Alegria, R. Colby, M. Rubinstein, D. Vlassopoulos, and S. Kumar, *Nature Communications* 2016, **7**, 11368.

82 G. A. Schwartz, J. Colmenero, and A. Alegria, *Macromolecules*, 2007, **40**, 3246.

83 F. Alvarez, A. Alegria, and J. Colmenero, *Phys. Rev. B,* 1991, **44**, 7306; F. Alvarez, A. Alegria, and J. Colmenero, *Phys. Rev. B,* 1993, **47**, 125.

A table of contents entry:

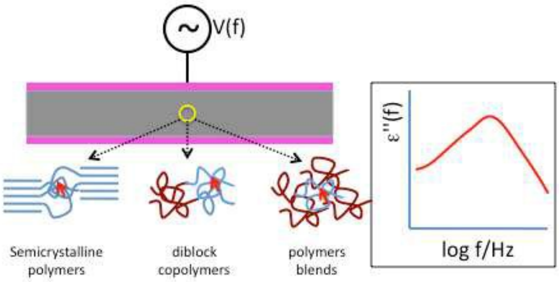

The effects of structural constrains on the main dielectric relaxation associated to segmental motions of polymer based materials is reviewed.